

Emerging Science Journal

(ISSN: 2610-9182)

Vol. 9, No. 5, October, 2025



Agarose-Based Antibacterial Films from *Gracilaria sp.*: Isolation, Characterization, and Metal Nanoparticle Incorporation

Ahyar Ahmad ^{1, 2}, Rahmaniah Zainuddin ¹, Budi Saksono ^{3, 4}, Sita Heris Anita ⁵, Deni Zulfiana ⁵, Riksfardini A. Ermawar ^{4, 6}, Rugaiyah Arfah ¹, Hasnah Natsir ¹, Harningsih Karim ⁷, Irmawati ⁸, Siti R. Ramli ⁹, Abdul Karim ^{1*}

Abstract

The incorporated metal nanoparticles in a polysaccharide-based film exhibit efficient antibacterial activity against harmful germs. However, previous studies have used a commercial polysaccharide for their film production. Therefore, this study aimed to develop a natural polysaccharide-based film extracted from the local algae Gracilaria sp. originating from Sinjai Regency, South Sulawesi, Indonesia. Firstly, the polysaccharide agarose was isolated and its properties compared with those of commercial agarose. A present low-cost isolation process produces agarose with 1.8% (w/w) of yield. Results also showed physicochemical properties similar to those of the commercial agarose. Secondly, the agarose-based antibacterial film was synthesized at 0, 0.5, and 1% glycerol concentrations. The synthesized film was incorporated with silver (Ag) and copper (Cu) nanoparticles (NPs). Morphological, mechanical, and physicochemical properties of the incorporated Ag-agarose and Cu-agarose films were characterized using Field Emission Scanning Electron Microscope (FESEM), Universal Testing Machine (UTM), and Fourier Transform Infrared Spectroscopy (FTIR), respectively. Results showed the film stiffness and tensile strength increased by incorporating either AgNPs or CuNPS. The interaction of AgNPs-agarose most likely involves physical bonds, while the interaction of CuNPs-agarose forms coordination bonds. An antibacterial test showed that the Ag-agarose nanocomposite inhibited the growth of Escherichia coli, Salmonella typhimurium, Staphylococcus aureus, Staphylococcus epidermidis, and Bacillus subtilis. In the meantime, Cu-agarose prevented the growth of Staphylococcus aureus. Overall, antibacterial activity was influenced by the interaction between metal nanoparticles and agarose, the concentration of metal nanoparticles, and the film's solubility. An agarose-based antibacterial film from Gracilaria sp. has the potential for use in various applications, including food packaging, pharmaceuticals, and other industries.

Keywords:

Agarose; Antibacterial Films; Gracilaria sp.; Metal Nanoparticles.

Article History:

Received:	04	February	2025
Revised:	10	August	2025
Accepted:	16	August	2025
Published:	01	October	2025

1- Introduction

Antibacterial films have been reported as an efficient means against harmful germs in many applications [1]. These films can be prepared using polysaccharides derived from various sources, such as macroalgae [2]. Several studies have

DOI: http://dx.doi.org/10.28991/ESJ-2025-09-05-03

© 2025 by the authors. Licensee ESJ, Italy. This is an open access article under the terms and conditions of the Creative Commons Attribution (CC-BY) license (https://creativecommons.org/licenses/by/4.0/).

¹ Department of Chemistry, Faculty of Mathematics and Natural Science, Hasanuddin University, Makassar 90245, Indonesia.

² Research and Development Centre for Biopolymers and Bioproducts, LPPM, Universitas Hasanuddin, Makassar 90245, Indonesia.

³ Research Collaboration Centre for Biomedical Scaffold, Universitas Gadjah Mada, and National Research and Innovation Agency, Yogyakarta, Indonesia.

⁴ Research Center for Biomass and Bioproducts, National Research and Innovation Agency BRIN, Cibinong Science Center, West Java 16911, Indonesia.

⁵ Research Center for Applied Microbiology, National Research and Innovation Agency BRIN, Cibinong Science Center, West Java 16911, Indonesia.

⁶ Research Collaboration Center for Biomass and Biorefinery between BRIN and Universitas Padjadjaran, Indonesia.

⁷ Department of Pharmacy, School of Pharmacy Yayasan Ma'bullo Sibatang, Makassar 90222, Indonesia.

⁸ Research and Development Centre for Biotechnology, LPPM, Universitas Hasanuddin, Makassar 90245, Indonesia.

⁹ National Institutes of Health, Institute for Medical Research, Infectious Disease Research Centre, Bacteriology Unit, Selangor, Malaysia.

^{*} CONTACT: abdulkarim@unhas.ac.id

shown that polysaccharides from microalgae, including cellulose, agar, chitosan, and agarose, have the potential as primary ingredients for antibacterial films due to their biocompatible, renewable, and environmentally friendly properties [2, 3]. Agarose, an essential component extracted from red algae, is widely used to prepare antibacterial films. This polysaccharide has unique properties, including hydroxyl-rich D-galactose groups on the polymer chain, which enable the formation of a stable matrix for incorporating antibacterial agents it, such as metal nanoparticles and plant extracts [4, 5]. Furthermore, polysaccharides from microalgae offer several advantages, including biodegradability, non-toxicity, antioxidant properties, and excellent film-forming ability [6].

Using agarose as a base material for antibacterial films generally involves incorporating antibacterial agents, such as metal nanoparticles or plant extracts, into the agarose matrix. Metal nanoparticles, including silver (AgNPs) and copper (CuNPs), exhibit strong antibacterial activity [7]. The antibacterial mechanism involves several processes, including the attachment of nanoparticles to the bacterial cell surface, which leads to cell wall destruction. Additionally, metal ions are released, interfering with various metabolic processes, such as respiration and protein synthesis. Furthermore, the nanoparticles produced reactive oxygen species, which are toxic and harmful to the integrity of the bacterial cell membrane. These synergistic interactions allow the metal nanoparticles to inhibit bacterial growth and kill bacteria effectively [8, 9].

Previous studies by Onofre-Cordeiro et al. (2018) [10] and Gholinejad & Jeddi (2014) [11] demonstrated that combining agarose as a film base with AgNPs and CuNPs yields promising antibacterial activity for biomedical applications. However, these studies employed commercial agarose, leaving the potential of agarose extracted directly from local sources—such as macroalgae—underexplored. This research gap presents an opportunity to evaluate agarose from local seaweeds abundant in Indonesia.

Gracilaria sp. was selected as a source of agarose due to its widespread cultivation in Indonesia, which offers a more economical and sustainable alternative. Moreover, it has a relatively high agarose and agaropectin content and exhibits superior gel strength compared to other types of agar. This high agarose content facilitates the formation of cross-links between polysaccharide chains, resulting in a strong and stable gel [12].

Despite its promising potential, the use of agarose derived from *Gracilaria sp.* combined with metal nanoparticles for the production of antibacterial films remains largely unexplored. Therefore, this study aimed to isolate and characterize agarose from *Gracilaria sp.* to synthesize nanocomposite films containing AgNPs and CuNPs. These films were prepared by solution casting, followed by the addition of metal nanoparticles and glycerol. The resulting nanocomposite films were physicochemically characterized—including surface morphology and functional groups—and evaluated for antibacterial activity against indicator microbes.

Furthermore, by combining the mechanical properties of agarose with the antibacterial effects of metal nanoparticles, the resulting films are expected to offer innovative solutions for various applications. The findings of this study are anticipated to provide valuable insights into the development of highly effective antibacterial films.

2- Materials and Methods

The flowchart of the research methodology that was used to achieve the study's aims is shown in Figure 1.

2-1-Preparation of Sample

Gracilaria sp. samples were collected from coastal areas of the marine ecosystem in Sinjai, South Sulawesi-Indonesia. The samples were from a local species commonly used as a primary source of agar. After collection, samples were rinsed with tap water to remove impurities. They were soaked in tap water for 24 hours at ambient temperature to reduce the built-in salt content and rewashed. This process was repeated until the samples were clean, as indicated by a paler color change. Afterwards, the samples were dried under the sun for approximately 72 h. The dried samples were ground into powder by a Universal Milling Machine (Krisbow, Indonesia). To homogenize the samples, particles were sieved through a 40 sieve. The sample powder was put into a plastic storage container for further processing. The powder was characterized by its components, including moisture content, ash content, extractive substances, holocellulose, α -cellulose, hemicellulose, acid-insoluble lignin (AIL), and acid-soluble lignin (ASL) [13].

2-2-Isolation of Agarose from Gracilaria sp.

A hundred (100) g of powder sample was steeped in 1.5 L of distilled water at room temperature for one night (10–12 h). After filtering the mixture, 1.5 L of a 10% (w/v) NaOH solution (Merck, Germany) was added, and the mixture was heated at 85 °C for 2 h. Alkaline (NaOH 10%) was formerly used to cure powder samples and to hydrolyze its agarose and agaropectin's link, which can boost the stability of the reaction that produces 3,6-anhydro-L-galactose [14]. The residue was then diluted with 500 mL of neutral pH distilled water. An All American 1925X Autoclave was used

to heat the mixture for 1.5 h at 120°C. After autoclaving, 0.1 g of activated charcoal (Merck, Germany) and 25 g of Celite 545 (particle size 0.02-0.1 mm, Merck, Germany) were added to the mixture while heating at 85°C. Activated charcoal and Celite 545 were added to extract agarose from agaropectin, yielding white agarose. The mixture was hot-filtered under vacuum at 60-80 psi. The extract was put into a mold and allowed to form a gel. The gel was frozen at -20 °C for 12 h. The gel was rethawed and dried at 50 °C. The dried agarose was ground and weighed. Figure 2 shows the agarose isolation process from *Gracilaria sp.* as described by Aslinda & Ahmad (2016) [15].

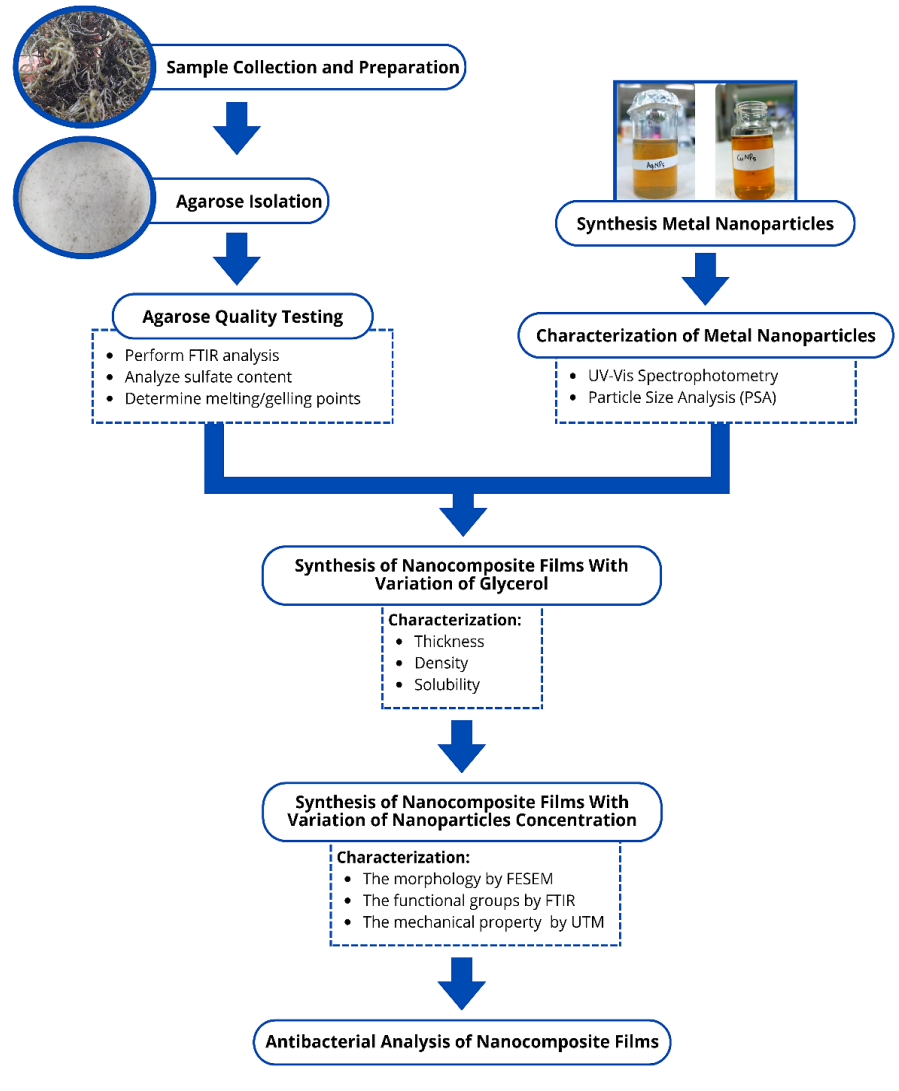


Figure 1. Flowchart of the methodology



Figure 2. The agarose isolation process

2-3-Agarose Characterization

Isolated agarose was characterized based on sulfate content, melting point, gelling point, and functional group analysis. The sulfate content was analyzed with a Shimadzu 1800 UV-Vis spectrophotometer at 420 nm using the turbidity method [16]. The gelling point was measured by cooling the agarose solution in a tilted test tube until a gel formed and recording the gelling temperature. The melting point was analyzed by heating the agarose gel until it melted and recording the melting temperature [17]. Agarose samples were made into KBr pellets and analyzed by Attenuated Total Reflectance Fourier Transform Infrared (ATR-FTIR) spectroscopy equipped with a UATR unit cell (spectrum two) (PerkinElmer Corporation, USA) to obtain an absorption spectrum indicating the functional groups [17, 18]. The characterization of *Gracilaria sp.* agarose was compared with commercial agarose (ThermoScientific, Lithuania) to determine the similarity of physicochemical properties based on sulfate content, melting point, gel formation point, and FTIR absorption spectrums.

2-4- Synthesis of AgNPs and CuNPs

AgNPs were produced via a reducing method using sodium citrate as the reducing agent. The citrate ions reduce the metal ions to metal atoms, which then aggregate to form nanoparticles [19]. The citrate ions also adsorb to the nanoparticles' surfaces, stabilizing them by preventing further aggregation. This method is simple, cost-effective, and produces stable and uniform silver nanoparticles with good biocompatibility. In a 100 mL Erlenmeyer flask, 50 mL of a 1 mM AgNO₃ (Merck, Germany) solution was heated to boiling to create AgNPs. Subsequently, 1% Na3C6H5O7 (Calbiochem, Israel) was added in 5 mL increments while stirring with a magnetic stirrer until the mixture turned yellow, indicating the formation of silver nanoparticles [20].

The synthesis of CuNPs used the chemical reduction method. Ascorbic acid is a natural reducing agent that can reduce copper ions to copper atoms. During the reaction, ascorbic acid ($C_6H_8O_6$) was oxidized to dehydroascorbic acid ($C_6H_6O_6$). Next, copper ions will be reduced to copper atoms. This technique yielded copper nanoparticles [21]. NaOH was added during synthesis as a stabilizing agent to prevent copper nanoparticle aggregation and to regulate the size of the nanoparticles [21]. L-ascorbic acid and NaOH were used in the reduction procedure to create CuNPs. A mixture was prepared by combining 10 mL of a 0.05 M CuSO₄ (Merck, Germany) solution with 0.5 mL of a 7.5 M NaOH solution. The mixture was swirled until a thick, light blue tint developed. A solution of L-ascorbic acid (Merck, Germany) with a concentration of 1.13M was added in a total volume of 1.2 mL. The orange color of the mixture indicates the formation of CuNPs [21].

The Shimadzu 1800 UV-Vis Spectrophotometer was used to evaluate the presence of AgNPs and CuNPs in colloidal solutions at wavelengths between 300 and 700 nm [18]. At the same time, a Malvern Panalytical Zetasizer Particle Size Analyzer Nano-S Zen 1600 was used to determine the nanoparticle size [22].

2-5-Synthesis and Characterization of Nanocomposite Films

Films were prepared by mixing 0.188 grams of agarose with 50 mL of deionized water. The mixture was heated to 100 °C until completely melted. Glycerol (Merck, Germany) was added as a plasticizer. Glycerol concentrations of 0, 0.5, and 1% (v/v) were added to the mixture. Metal nanoparticles at a 30% (v/v) concentration in the mixture were added and deposited in the mold. The mold was heated in an oven (Memmert UF 160, Germany) at 40 °C for approximately 16 hours [10]. The thickness, density, and solubility of the resulting films were characterized as described by Ediyilyam et al. (2021) [23]. Additionally, the morphology of the selected sample, i.e., a sample containing 1% glycerol and 30% nanoparticles, was further analyzed using a Field Emission Scanning Electron Microscope (FESEM) Thermo Scientific Quattro S [24]. The mechanical property of the selected sample, i.e., its tensile strength, was measured in accordance with ASTM D882-18 [25] by Universal Testing Machine (UTM) Shimadzu AGS-X series 10 kN with TrapeziumX application. The chemical composition's functional group of the selected sample was further analyzed by Fourier Transform Infrared Spectroscopy (FTIR) Attenuated Total Reflectance (ATR) 4000 Perkin Elmer [17]. The mold samples containing 1% glycerol and various concentrations of nanoparticles (10, 20, and 30%) were further tested for antibacterial activity.

2-6-Antibacterial Analysis of Nanocomposite Films

The agar diffusion was used to analyze the antibacterial activity of nanocomposite films [26]. Antibacterial tests were performed with positive and negative control tests for evaluation. The positive control test used films added with the antibiotic chloramphenicol (Kimia Farma, Indonesia). Agarose film without added metal nanoparticles was used as the negative control. The test was done on the following bacteria species: *Pseudomonas aeruginosa* ATCC 15442 and *Escherichia coli* ATCC 8739, which were isolated from the IPBCC (IPB Culture Collection). *Staphylococcus aureus* ATCC 29213, *Staphylococcus epidermidis, Bacillus subtilis* FNCC 0622, and *Salmonella typhimurium* FNCC 00157 were purchased from the Indonesian retail market.

In a 100 mL Erlenmeyer, 50 mL sterile nutrient broth (Merck, Germany) was inoculated with one colony of bacteria from an NB plate and incubated in a shaking incubator at 110 rpm and 37 °C for 24 h. After the incubation period finished, as much as 1% (v/v) of each bacterial inoculum containing 10⁷-10⁸ CFU/mL of bacterial cells was put into sterile nutrient agar (Merck, Germany) medium and homo and mixed until homogeneous using a vortex mixer Thermo Scientific. Twenty milliliters of the medium containing the bacterial culture were poured into the sterilized petri plates and allowed to be set. A film sample measuring 5 millimeters in diameter was placed on the agar surface. The plates were placed in an incubator for 24 h at 37°C. The inhibitory zone diameter (mm) was measured every 2 h by determining the clear area surrounding the samples.

3- Results and Discussion

3-1-Analysis of the Chemical Components of Gracilaria sp.

Gracilaria sp. was used as a source of agarose, and its chemical composition needed to be tested first to assess the quality and purity of the raw material. These chemical component tests ensured that Gracilaria sp. was suitable for agarose extraction. Table 1 shows the chemical components of Gracilaria sp. tested in this study. Gracilaria sp. has a water content of $15.2 \pm 0.44\%$ (w/w), almost the same as the water content in previous research using the seaweed Gracilaria verrucosa, namely 16.29 ± 0.21 (w/w) [14]. This low water content indicates that the Gracilaria sp. has dried well.

	•	•
Chemical Component	Total Percent (%)	SD
Moisture	15.2	0.44
Ash	10.0	0.08
Extractive content	20.8	0.80
Acid Insoluble Lignin (AIL)	0.2	0.11
Acid Soluble Lignin (ASL.)	8.9	1.08
holocellulose	15.8	1.09
α-cellulose	8.9	0.51
Hemicellulose	6.8	0.58

Table 1. The chemical component of Gracilaria sp.

The research results showed that after drying, the moisture content of *Gracilaria sp.* was $15.2 \pm 0.44\%$ (w/w). According to the Indonesian National Standard, the maximum moisture content of dried *Gracilaria* seaweed was 18% [27]. Moisture content exceeding 20% causes the *Gracilaria sp.* sample to be more prone to damage, thereby reducing the quality of the resulting agar. The lower the seaweed's moisture content, the slower the degradation of quality caused by chemical processes and enzymatic and microbial activity. However, when the moisture content is shallow, the agar may become too dry and brittle [28].

By reducing moisture content to the recommended threshold, the drying process can minimize the risk of material damage and optimize the physicochemical properties of the resulting agarose. Overall, these positive results demonstrate the efficacy of the drying technique used in producing high-quality raw materials for agarose production.

3-2- Agarose Isolation

Agarose was successfully isolated from *Gracilaria sp* using a cost-effective process method. From separating 250 g of seaweed powder, 4.51 g of white agarose was obtained, divided with 1.8% (w/w) agarose. The yield of agarose from *Gracilaria sp*. was 1.8% (w/w). The yield obtained was greater than that reported in a similar study using the same method, i.e., 0.65% (w/w) for *Euchema cottoni* seaweed [15]. However, this yield was lower than that reported for other studies on *G. dura* seaweed, i.e., 23% (w/w) [29]. These results may be due to the extraction process, which was repeated only once, leaving some agarose unextracted. Therefore, improvements in the extraction process can increase the yield of agarose produced.

Several variables affect agarose yield, including seaweed type, extraction process, and storage conditions. Other factors that may affect agarose yield include the age and size of the algae, the season of harvest, and rainfall in the growing area. In addition, the purity of the extracted agarose, as well as any impurities present in the algae or in the extraction process, can affect the agarose concentration in the final product [30]. For example, optimal conditions for extracting agar from *Gracilaria salicornia* seaweed were observed at a NaOH concentration of 30%, an alkali pretreatment time of 2 h, and an extraction temperature of 120 °C [31].

3-3-Characterization of Agarose

The agarose from *Gracilaria sp.* was characterized by its physical and chemical properties, which were compared with those of commercial agarose. Agarose from *Gracilaria sp.* was also analyzed for sulfate content to determine its purity. Test results for sulfate levels from agarose from *Gracilaria sp.* and other sources are shown in Table 2. In this study, the sulfate levels of agarose isolated from Gracilaria sp. were $0.29 \pm 0.0\%$.

Agarose Sources	Sulphate Content (%)	References
Gracilaria sp.	0.29 ± 0.0	In this study
Gracilaria dura	0.25	[29]
Euchema cottoni	0.26	[15]
Thermo Scientific	0.1	Cat No: R0492

< 0.30

Cat No: A9668

Sigma Aldric

Table 2. Comparison of sulfate content of agarose with commercial agarose and different species

Compared to commercial agarose, the isolated agarose has a sulfate content that is not significantly different from that of Sigma agarose. However, the sulfate content is still higher than that of other commercial agaroses, such as Thermo Scientific agarose. The presence of sulfate in agarose indicates the presence of agaropectin remaining after the sulfate separation process. The lower the sulfate content in agarose, the higher the purity of the agarose obtained [12]. Additionally, the sulfate content demonstrates agarose's neutral properties and gel strength. As sulfate content decreases, agarose becomes increasingly neutral. Likewise, decreasing sulfate levels can increase gel strength [12]. Therefore, the 0.29% sulfate content suggests that the isolated agarose, despite not having optimal purity, still meets the basic requirements for standard biochemical and microbiological applications.

The low sulfate test results signify that the purity level of the obtained agarose was reasonably high and met good agarose standards. However, further research is needed to optimize the agarose isolation process from Gracilaria sp. and to determine agarose's functional properties that meet industrial standards. These efforts are essential to enhance the quality and purity of agarose as a raw material for advanced materials. Optimizing the isolation process can yield agarose that meets pharmaceutical and biomedical grade specifications.

The physical properties analyzed were gel formation temperature and melting point. The results of gel point and melting point tests are shown in Table 3. The agarose from *Gracilaria sp.* had a gel point of 36.5°C, slightly higher than the commercial agarose at 35°C. The melting point analysis showed that the agarose from *Gracilaria sp.* had a melting point of 91°C, slightly higher than that of the commercial agarose (90 °C).

Table 3. The comparison of the physical properties of extracted agarose with commercial agarose and different species

Agarose from	Melting Point (°C)	SD	Gelling Point (°C)	SD	References
Commercial	90	0.5	35	0.5	In this study
Gracilaria sp	91	1.7	36.5	0.5	In this study
Gracilaria dura	-	-	35	0.5	[21]
Euchema cottoni	96	-	-	-	[12]
Gracilaria verrucosa	90	0	34	0	[11]

The comparison of the physical properties of isolated agarose and commercial agarose showed that the physical properties of isolated agarose were almost similar to those of commercial agarose. Agarose from *Gracilaria sp.* had a gelling point of 36.5°C, higher than commercial agarose, which was 35°C. One of the main variables affecting the gel formation temperature is agarose concentration, with higher concentrations resulting in higher gel formation temperatures. Contaminants can also influence the temperature at which agarose starts to form a gel. The presence of impurities in agarose can increase the gel formation temperature. For example, salts can raise the gel-forming temperature by altering the gel's ionic strength. Polysaccharides can also increase the gel formation temperature by disrupting the formation of agarose fibers [17, 30].

The melting point analysis results for isolated agarose were 91°C, higher than those for commercial agarose (90 °C). Many factors can affect the melting point of agarose, including its concentration and purity. Agarose gel concentration can also affect the melting point, with higher concentrations producing higher melting points. Agarose purity also affects the melting point. The higher the impurity levels, the lower the agarose melting point [29].

The slight differences in the melting point and gel strength of agarose from *Gracilaria sp.* may be due to impurities and the agarose's purity level. These results agree with the sulfate content test, in which agarose from Gracilaria sp. had slightly higher sulfate content, indicating that its purity was slightly lower than that of commercial agarose. This result influences the differences in the physical properties of the agarose.

The chemical structure of agarose can be identified by infrared (IR) spectrum analysis, which records specific absorption bands. The FTIR spectrum of isolated agarose was used to confirm its identity with commercial agarose (Thermo Scientific). FTIR analysis showed a spectrum similar to that of *Gracilaria sp.* and commercial agarose. The FTIR spectrum of the agarose and the identified bonds are displayed in Figure 3 and summarized in Table 4. FTIR analysis showed a spectrum similar to that of agarose from *Gracilaria sp.* and to that of commercial agarose.

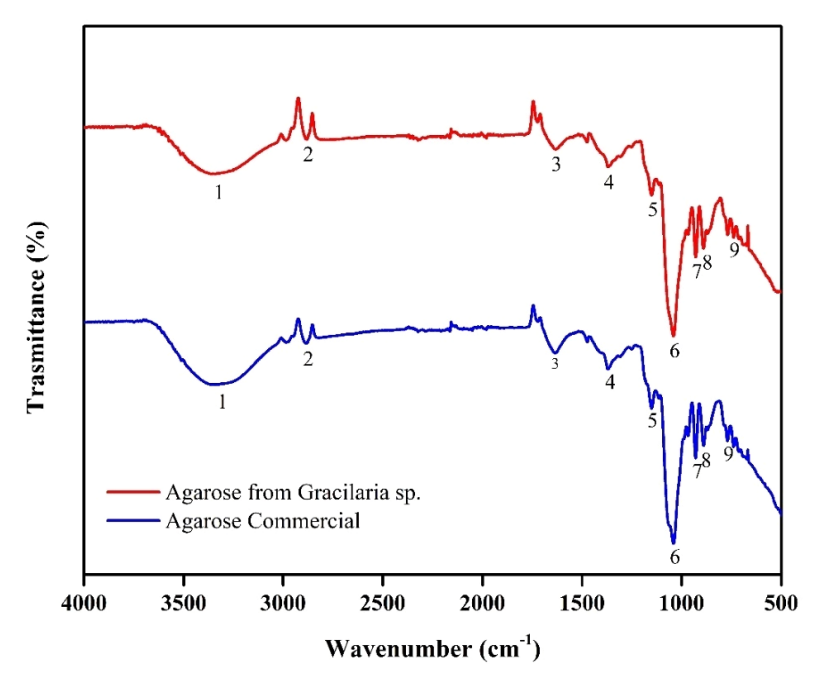


Figure 3. FTIR pattern result of commercial agarose and agarose from Gracilaria sp.

Table 4. Assignments of the FTIR spectrum pattern of the agarose from Gracilaria sp. and Commercial

No.	Wave number (cm ⁻¹)		Identification of Functional	
	Gracilaria sp.	Commercial	Groups	
1	3318	3324	O-H stretching	
2	2885	2883	C-H stretching	
3	1634	1634	C=O streaching	
4	1363	1354	S=O stretching	
5	1150	1149	C-O-C streaching	
6	1048	1047	C-O stretching	
7	929	929	O-H bending	
8	887	885	C-H bending	
9	769	769	C-O bending	

Both agaroses exhibit a broad absorption band at 3320 cm-1, corresponding to the O-H stretching vibration. This O-H group originates from the hydroxyl groups on the galactose units and on 3,6-anhydro-L-galactose, which constitute agarose. The absorption band at wavenumber 2880 cm⁻¹ indicates the presence of C-H bonds in alkyl and methyl structures derived from the agarose carbon backbone. The medium intensity absorption band at 1634 cm⁻¹ corresponds to the stretching vibration of the carbonyl group (C=O) in the galactose units. The presence of sulfate groups in agarose is indicated by an absorption band at 1363 cm-1, corresponding to the sulfate ester group. The absorption band at 1150 cm-1 corresponds to the C-O-C bonds in the glycosidic linkages between the galactose units that make up agarose. The presence of these glycosidic bonds is crucial, as they are involved in the formation of agarose polymer chains [15, 32-35].

3-4-Synthesis and Characterization of Metal Nanoparticles

The synthesized AgNPs were characterized using UV-vis spectroscopy and PSA. Figure 4-a shows the results of the AgNPs characterization using UV-vis spectrophotometry. The characterization results showed a peak at 429.5 nm, confirming the presence of AgNPs. Meanwhile, the PSA characterization showed that the silver nanoparticles had an average particle size of 106.6 nm, with 100% of the particles within the detection range. The polydispersity index was also 0.48, indicating that the AgNP sample was homogeneous with a narrow particle-size distribution.

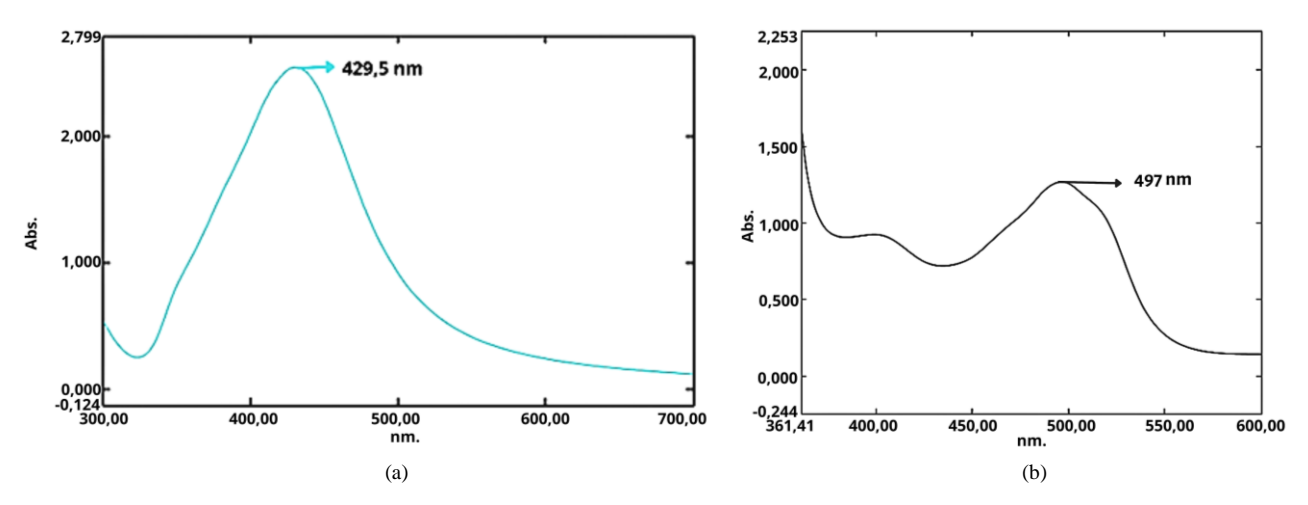


Figure 4. The outcomes of the UV-Vis spectrophotometric characterization of (a) AgNPs, (b) CuNPs

The characterization results showed a peak at 429.5 nm. Metal nanoparticles have unique optical properties due to their tiny size, allowing their free electrons to resonate with incoming light and reflect light with specific colors. The specific absorption peak for AgNPs is around 400 nm wavelength. The presence of an absorption band around 400 nm is an initial indicator of AgNP formation [7]. Characterization by UV-Vis spectrophotometry confirmed the formation of AgNPs, as evidenced by an absorption peak at 429.5 nm. This result agrees with previous studies reporting absorption peaks ranging from 411.4-432.7 nm [36] and 421-431 nm [37].

PSA also characterized silver nanoparticles (AgNPs) to determine their particle size. PSA characterization showed that AgNPs have an average particle size of 106.6 nm (100%) and a polydispersity index of 0.4773. A polydispersity index value of less than 0.5 indicates a relatively narrow nanoparticle size distribution or a homogeneous sample [38]. According to the research conducted by Khatoon et al. (2013) [39], silver nanoparticles were synthesized using sodium citrate and measured 14–30 nm. Meanwhile, Tessema et al. (2023) [40] synthesized silver nanoparticles using sodium citrate and an African leaf extract, yielding sizes of 63.08 nm and 38.47 nm, respectively. Based on comparisons with these studies, the nanoparticles synthesized in this study are larger than those reported previously. However, their size still remains within the nanoscale.

The characterization of CuNPs results using UV-vis spectrophotometry showed a peak at a wavelength of 497 nm, which indicates the formation of CuNPs (Figure 4-b). CuNPs were also characterized using PSA to see the particle size of CuNPs formed. Copper nanoparticles had particle sizes of 31.14 nm (99.4%) and 121 nm (0.06%). The polydispersity index value was 0.48, indicating that the sample was homogeneous.

Characterization of CuNPs using a UV-Vis spectrophotometer showed a distinct absorption peak at 497 nm, confirming their formation. This absorption peak corresponds to the SPR of the synthesized CuNPs in the 400-700 nm range, consistent with the literature [41]. Fundamentally, SPR arises from the collective oscillation of conduction band electrons on the metal nanoparticle surface interacting with the electric field component of the impinging light wave [7].

Further characterization using PSA showed an average CuNP size of 31.14 nm with a relatively narrow size distribution, with 99.4% in that range and only 0.06% at 121 nm. This size meets the nanoparticle criteria of less than 100 nm and falls within the literature range of 10-158 nm [42]. The low polydispersity index value of 0.4824 indicates a uniform size distribution among the nanoparticles.

3-5-Synthesis of Nanocomposite Films

3-5-1- Fabrication and Characterization of Nanocomposite Films with Variation of Glycerol

The synthesis of antibacterial was carried out by the casting solution method. All nanocomposite materials were dissolved in a solvent (distilled water) while being heated and stirred [10]. The mixture was then molded in a petri dish and dried to form a film. Antibacterial films were prepared with varying amounts of glycerol as a plasticizer. Figure 5 shows the results of antibacterial films with varying glycerol concentrations.

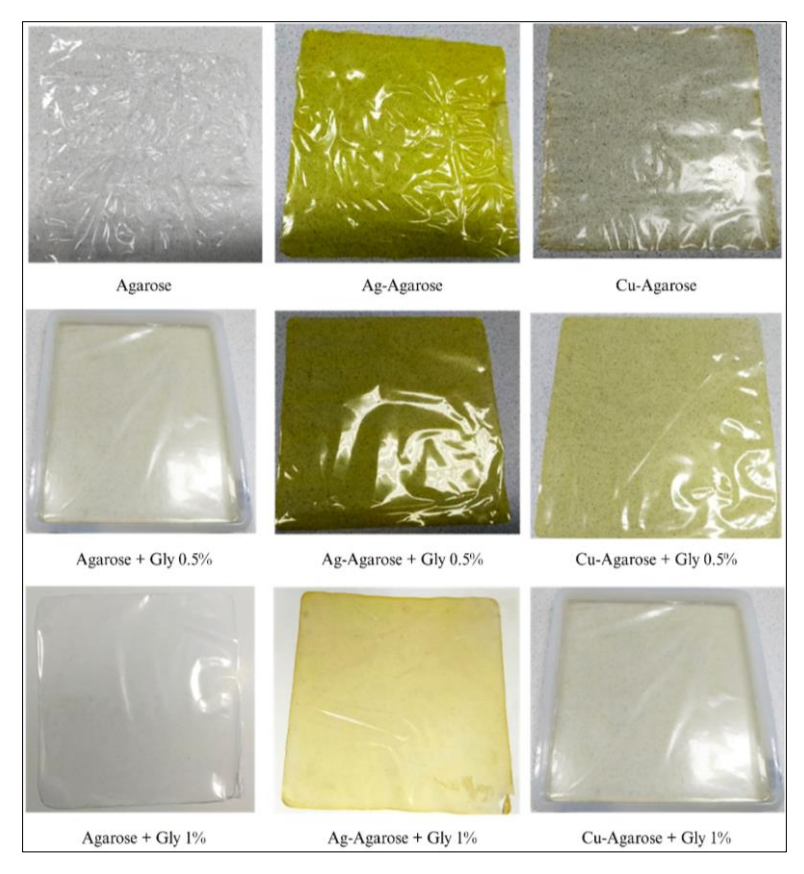


Figure 5. Nanocomposite films with variation of glycerol

Variations in glycerol addition affect the characteristics of the films formed. The film without glycerol addition showed an uneven surface, with many wrinkles. The second film, which contained 0.5% glycerol addition, significantly improved. Glycerol contributed positively to the film's surface, resulting in a smoother finish and reducing the likelihood of wrinkles. These characteristics are similar to those of the film with 1% glycerol, in which the surface becomes flat without wrinkles.

Thus, it can be concluded that adding glycerol to the film formulation improves film characteristics, particularly the smoother, flatter surface. This result was in accordance with previous research. The addition of glycerol can make the film surface smoother, homogeneous, and better distributed [43].

The antibacterial film was analyzed to determine its thickness, density, and water solubility, which are its main characteristics. This test was conducted to understand the impact of glycerol addition on the film characteristics. Thickness analysis focuses on the physical dimensions of the film, while density provides insight into mechanical strength and potential as a bacterial barrier. Evaluation of water solubility helps understand the release of antibacterial agents on the film. These test results provide crucial information on the effect of glycerol on the functional properties of antibacterial films, which is vital for designing optimal formulations. Table 5 shows the characteristics of antibacterial films with varying glycerol addition.

Table 5. Characteristics of nanocomposite films with varying glycerol addition

Film	Thickness (mm)	Density (g/cm³)	Solubility (%)
Agarose	0.03 ± 0.01	0.67 ± 0.01	8.94 ± 0.34
Agarose + Gly 0.5%	0.05 ± 0.01	0.80 ± 0.03	22.34 ± 0.38
Agarose + Gly 1%	0.06 ± 0.01	0.90 ± 0.02	59.58 ± 1.39
Ag-Agarose	0.04 ± 0.01	0.76 ± 0.02	20.94 ± 0.92
Ag-Agarose + Gly 0.5%	0.06 ± 0.01	0.96 ± 0.01	36.13 ± 1.14
Ag-Agarose + Gly 1%	0.09 ± 0.01	1.27 ± 0.01	59.37 ± 0.40
Cu-Agarose	0.04 ± 0.01	0.80 ± 0.02	43.39 ± 0.54
Cu-Agarose + Gly 0.5%	0.05 ± 0.01	0.86 ± 0.02	55.24 ± 0.31
Cu-Agarose + Gly 1%	0.08 ± 0.01	0.92 ± 0.01	69.34 ± 0.14

The results of the antibacterial film thickness test, with varying glycerol additions, showed a trend of increasing thickness with increasing glycerol addition. These results are consistent with previous research showing that the increase in antibacterial film thickness due to the addition of glycerol is associated with greater total solids content in the film, which, in turn, results in greater film thickness [44, 45]. The antibacterial film had a thickness of 0.03-0.08 mm. These results are consistent with the JSA (2019) [46] standard, which requires packaging to have a maximum thickness of 0.25 mm. The films made were included in the thin plastic sheeting category because they produced a thickness of less than 1 mm [47].

The film's density indicates its compactness. The density test results show that the film's density increases with the addition of glycerol (Table 3). The increase in density was due to the addition of glycerol, which increased the total solid content and thus the film density. The density affects the film's antibacterial activity. Increasing the film's density increases the distance between molecules, inhibiting the diffusion of nutrients and oxygen, which are essential for bacterial growth. In addition, high film density creates a more compact structure, making it more difficult for bacteria to penetrate [48].

The film solubility test is essential. Increased film solubility will accelerate the release of metal ions into the liquid medium, thereby improving antibacterial activity. Glycerol acts as a plasticizer, increasing the flexibility of the agar matrix and making the film more soluble. The solubility test results showed that the highest solubility was in the film with 1% glycerol addition formulation. The incorporation of glycerol as a plasticizer significantly increases the solubility of antibacterial films by disrupting polymer chain interactions, reducing intermolecular forces, and increasing mobility, thereby allowing greater water permeation into the matrix [49].

The antibacterial test used agar diffusion with *Staphylococcus aureus*. This bacterium was chosen because it's commonly found in foods. The zone of inhibition formed around the film indicates antibacterial activity. This area is often referred to as the zone of inhibition or the area where bacteria cannot grow [50]. Figure 6 shows the antibacterial activity of the films with varying glycerol addition.

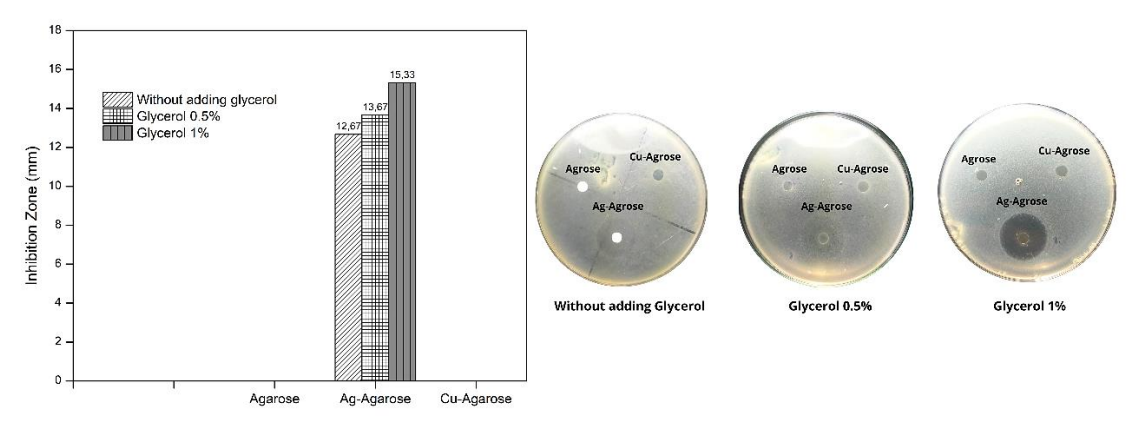


Figure 6. The activity of antibacterial with the variation of glycerol concentrations

The antibacterial test results indicate that agarose film samples without added metal nanoparticles exhibit no antibacterial activity against Staphylococcus aureus, as expected for the negative control. However, films containing AgNPs exhibit antibacterial activity, as evidenced by inhibition zone diameters of 12.67 mm, 13.67 mm, and 15.33 mm for films without glycerol, with 0.5% glycerol, and with 1% glycerol, respectively. The increase in the inhibition zone with increasing glycerol concentration indicates enhanced antibacterial activity, possibly due to improved film solubility and metal ion release.

Glycerol is commonly used as a plasticizer to impart flexibility to films by disrupting polymer interactions and facilitating chain mobility [49, 51]. This interaction increases film solubility and enhances the diffusion of active agents, such as metal ions, into the surrounding medium. The highest solubility achieved with 1% glycerol enables faster, more complete diffusion of metal ions, thereby enhancing their availability for antibacterial activity compared to films with lower or no glycerol. Higher solubility also correlates with a faster release rate and lower retention of active agents in the film matrix [52]. Therefore, the superior antibacterial performance of the 1% glycerol film may be slightly reduced over time due to the faster depletion of metal ion stocks. Optimal glycerol concentration can balance solubility and release with active agent retention.

From the results of nanocomposite film characterization with varying glycerol content, the best film formulation in terms of thickness, density, film solubility, and antibacterial activity is the 1% glycerol film. These results can provide preliminary information for the manufacture of agarose-based antibacterials with varying concentrations of metal nanoparticles.

3-6-Characterization of Nanocomposite Films

The film formulation with the best physical properties, namely adding 1% glycerol and 30% metal nanoparticles, produces antibacterial films that will be characterized further. Film characteristics were analyzed using mechanical properties, morphology, and functional groups.

3-6-1- Mechanical Properties of Nanocomposite Film

The mechanical properties of the nanocomposite films are presented in Table 6. The pure agarose film exhibits low elastic modulus and tensile strength values, being 0.028 MPa and 3.08 MPa, respectively. These results indicate that the pure agarose film is brittle and has weak mechanical properties. The results of the mechanical property tests show that incorporating AgNPs or CuNPs increases the values of Young's modulus and tensile strength. Adding AgNPs increases Young's modulus and tensile strength to 0.323 MPa and 9.98 MPa, respectively. Meanwhile, adding CuNPs also improves these properties, increasing Young's modulus and tensile strength to 0.058 MPa and 5.82 MPa, respectively, although not as significantly as AgNPs. These results suggest that incorporating metal nanoparticles increases film stiffness and tensile strength.

Film	Modulus Young (MPa)	Tensile Strength (MPa)	Elongation of break (%)
Agarose	0.028 ± 0.003	3.08 ± 0.63	13.72 ± 3.49
Ag-Agarose	0.323 ± 0.087	9.98 ± 1.39	9.01 ± 2.47
Cu-Agarose	0.058 ± 0.014	5.82 ± 1.32	14.62 ± 2.54

Table 6. Mechanical properties of nanocomposite films

The findings of this study are consistent with those reported by Onofre-Cordeiro et al. (2018) [10] and Bang et al. (2022) [53], who synthesized agarose-based films incorporating metal nanoparticles. In their work, the addition of metal nanoparticles significantly increased the mechanical strength of the composite films. This enhancement was attributed to the interaction between the agarose matrix and the metal nanoparticles via physical forces, such as van der Waals interactions, thereby improving interfacial adhesion. However, incorporating silver nanoparticles (AgNPs) decreased film flexibility, as evidenced by a reduction in elongation at break to 9.01%. This indicates that while the nanoparticles reinforce the film, they also restrict the mobility of the polymer chains, resulting in a stiffer, less flexible material. These results align with those of Bang et al. (2022) [53], who observed increased film stiffness accompanied by diminished polymer chain mobility, ultimately reducing flexibility.

3-6-2- Morphology of Nanocomposite Films

The SEM-EDX test results are shown in Figure 7. The SEM test results showed that the agarose film without nanoparticle addition had the smoothest surface among the other films. However, EDX analysis confirmed carbon (C) and oxygen (O) as the primary components of agarose, with some silica contamination from the fabrication process [10].

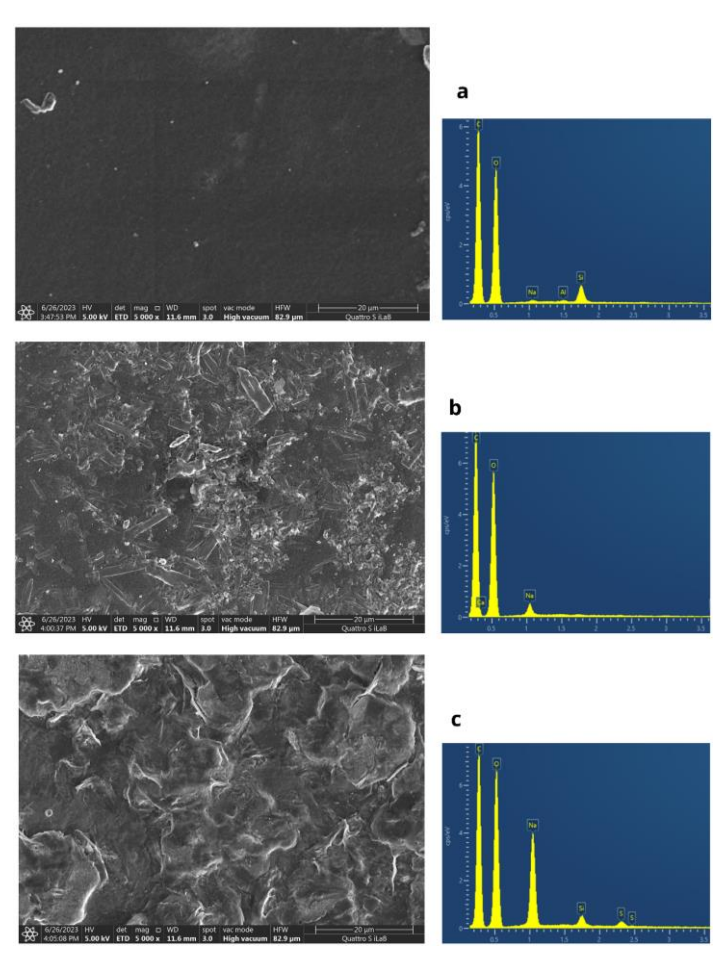


Figure 7. SEM-EDX test results of antibacterial films (a) agarose alone, (b) Ag-agarose, (c) Cu-agarose

The Ag-agarose film displayed an uneven surface with small rods and spherical-shaped crystalline structures, indicating AgNP entrapment. The interaction between AgNPs and agarose disrupted the polymer chain arrangement, leading to surface irregularities [53]. Meanwhile, SEM analysis of the Cu-agarose film revealed an irregular morphology with pores, possibly resulting from interactions between CuNPs and agarose hydroxyl groups. This interaction may have disrupted the agarose network, creating voids [54].

EDX failed to detect silver and copper due to their low concentration, below the instrument's detection limit (<1%). This finding is consistent with the study by Onofre-Cordeiro et al. (2018) [10], which reported the absence of detectable nanoparticle absorption peaks in EDX analysis for similar reasons. The limited nanoparticle content in the film may affect its antibacterial performance, as lower AgNP concentrations could reduce the release of antimicrobial ions. Therefore, optimizing the fabrication process is necessary. Improving nanoparticle dispersion, increasing their concentration, and refining synthesis conditions could enhance film homogeneity, mechanical properties, and antibacterial effectiveness, making the material more suitable for biomedical and industrial applications

3-6-3- Functional Groups of Nanocomposite Films.

The FTIR test results are shown in Figure 8. The FTIR results showed similarities in absorption peaks between agarose film and Ag-agarose. Meanwhile, the Cu-agarose film had a very different absorption spectrum. Interactions between metals and agarose may cause differences in FTIR results [10, 17, 53].

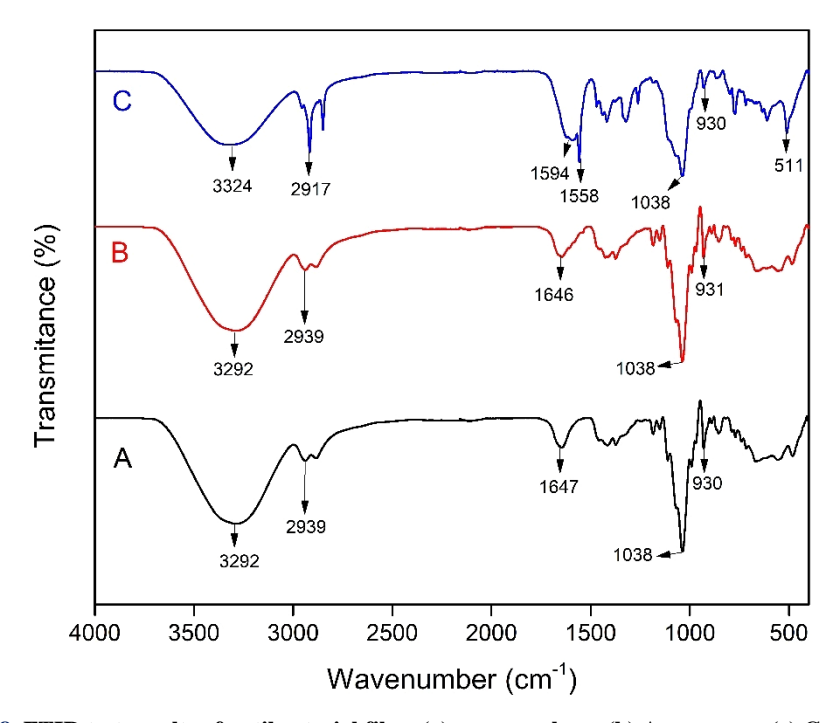


Figure 8. FTIR test results of antibacterial films (a) agarose alone, (b) Ag-agarose, (c) Cu-agarose

The IR spectrum of the pure agarose film exhibited characteristic absorption peaks of agarose functional groups. A broad peak at 3292 cm⁻¹ corresponded to O-H stretching vibrations, while the peak at 2939 cm⁻¹ was due to C-H stretching. The peak at 1646 cm⁻¹ originated from C=O vibrations in galactose, and peaks at 1038 cm⁻¹ and 930 cm⁻¹ were associated with sulfate ester groups and 3,6-anhydro-L-galactose, respectively [10, 53, 55].

The IR spectra of agarose and Ag-agarose films were similar, indicating no new chemical bonds formed between agarose and AgNPs. This suggests that AgNPs were physically trapped in the agarose matrix. The findings align with previous studies, Onofre-Cordeiro et al. (2018) [10] and Bang et al. (2022) [53], supporting the goal of producing a nanocomposite film with physical interactions. According to Rhim et al. (2013) [55], weaker physical interactions facilitate nanoparticle release into the environment, enhancing antibacterial activity but potentially reducing film stability.

In contrast, the FTIR spectrum of the Cu-agarose film showed significant differences. A shift from 1646 cm⁻¹ to 1594 cm⁻¹ and a new peak at 1554 cm⁻¹ indicated coordination bonding between Cu²⁺ ions and oxygen from hydroxyl groups [17]. Additionally, an absorption peak at 511 cm⁻¹ confirmed Cu-O bond formation [56]. The coordination bond likely restricted polymer chain mobility, reducing glycerol's plasticizing effect, as evidenced by an O-H peak shift from 3291 cm⁻¹ to 3324 cm⁻¹ [57].

Based on the SEM-EDX and FTIR characterization results, the reaction mechanism in the nanocomposite film is illustrated in Figure 9.

Figure 9. Illustration of the reaction mechanism that occurs in the nanocomposite film (a) Ag-agarose, (b) Cu-agarose

3-7-Antibacterial Activity of Nanocomposite Films

The antibacterial test was conducted to assess the effect of metal nanoparticle concentration on the film's antibacterial activity. The film formulation was based on adding 1% glycerol and 10-30% metal nanoparticles. The antibacterial activity was determined by measuring the inhibition zones around the nanocomposite films, which were represented by clear areas where bacterial growth was prevented [50]. The antibacterial results of the nanocomposite films are shown in Figure 10. Results showed that Ag-Agarose nanocomposite films exhibited broad-spectrum antibacterial activity against both Gram-positive (*Staphylococcus aureus, Staphylococcus epidermidis, Bacillus subtilis*) and Gram-negative bacteria (*Escherichia coli, Salmonella thypimurium*). In contrast, Cu-Agarose films only inhibited the growth of *Staphylococcus aureus* bacteria. This result indicates that while Cu has antibacterial activity against certain bacteria, adding AgNPs can enhance the broad-spectrum antibacterial activity of the nanocomposite films.

The antibacterial efficacy of Ag-Agarose films on Staphylococcus aureus was further examined at varying AgNPs concentrations and incubation times. Results showed the largest inhibition zone of 15.3 ± 0.6 mm formed at 30% AgNPs concentration after 8 h of incubation. This inhibition zone falls under the category of bacterial solid growth suppression. Films containing 10% and 20% AgNPs also exhibited potent inhibition of Staphylococcus aureus, with inhibition zone sizes of 12.7 ± 0.6 mm and 13.7 ± 0.6 mm, respectively. However, the antibacterial activity of Ag-Agarose films on Staphylococcus aureus decreased after more than 8 h of incubation. Meanwhile, Cu-Agarose films inhibited Staphylococcus aureus growth at 20% and 30% CuNPs concentrations. No inhibition zone was observed at 10% CuNPs concentration. The most significant inhibition zone, 10 ± 0.4 mm, was observed at a 30% CuNPs concentration after 8 h of incubation.

This study utilized positive and negative controls to obtain more accurate assessments of antibacterial activity. The positive control provides a benchmark for the antibacterial efficacy of the tested nanocomposite films by using a known antibacterial agent as a reference. Meanwhile, the negative control, which contains no antibacterial compounds, helps identify and eliminate variables other than the nanocomposite films that may cause inaccurate inhibitory results. Antibacterial diffusion tests on the negative control showed no inhibition zone formation, indicating the absence of antibacterial agents. This result confirms that the negative control will not contribute to or interfere with the analysis of metal nanoparticle antibacterial activity [58].

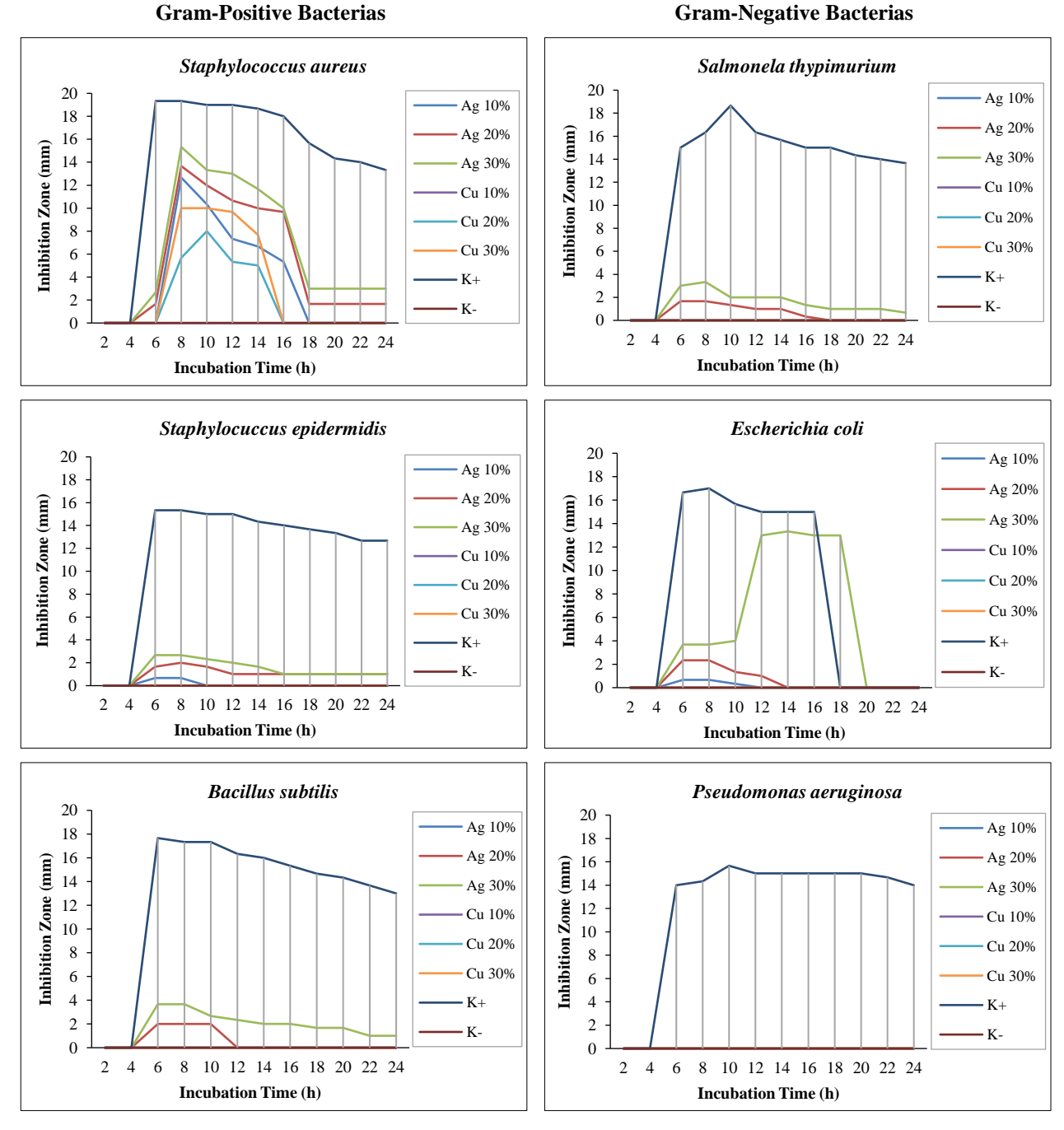


Figure 10. Antibacterial Activity of the Nanocomposite Film Against Several Bacteria Test for 24 Hours of Incubation

The antibacterial test results demonstrated that Ag-agarose and Cu-agarose nanocomposite films effectively inhibit the growth of Gram-positive and Gram-negative bacteria strains. However, the films showed greater efficacy against Gram-positive bacteria overall. This variance in efficacy against different bacterial species is attributable to each bacterial species' unique cell wall structure and outer membrane composition [59]. The cell walls of Gram-positive bacteria usually consist of a thick peptidoglycan layer, which metal nanoparticles can more easily penetrate. In contrast, Gram-negative bacteria have an additional outer membrane structure surrounding the peptidoglycan. This outer membrane comprises tightly packed phospholipids, lipopolysaccharides, and membrane proteins, forming a denser, low-permeability layer that provides a more effective barrier against the penetration of antimicrobial agents [59, 60]. Considering these factors, the nanocomposite films exhibit more potent antibacterial activity against Gram-positive bacteria than against Gram-negative strains.

Further antibacterial activity testing showed that Ag-agarose films exhibit greater bacterial growth inhibition than Cu-agarose films. This superior performance is attributable to the high reactivity and proneness of silver ions released from nanoparticles to interact with and damage intracellular components, effectively preventing bacterial reproduction. The presumed mechanism of bacterial cell damage by Ag-agarose involves silver ions readily binding to the thiol (-SH) groups of essential proteins and enzymes within bacterial cells [9]. As a soft acid, silver ions (Ag⁺) have a higher tendency to form coordination bonds with soft bases like the -SH groups. In comparison, copper (Cu²⁺) ions are classified as

intermediate borderline acids and thus have a lower binding affinity towards these cell targets. This selective binding of Ag⁺ to bacterial proteins inactivates enzyme activity and disrupts cellular metabolism, eventually preventing reproduction and killing the bacterial cells [60].

Moreover, prior characterization results influence the high antibacterial activity of Ag-agarose films. Physical interaction between AgNPs and agarose facilitates their release into the bacterial media. A weaker physical interaction strength leads to more readily released Ag+ into the environment and inhibits bacterial growth. In contrast, Cu-agarose films likely exhibit strong coordination bonding between CuNPs and the hydroxyl groups of the agarose polymer. This sufficiently strong chemical bond restricts and decelerates the release of CuNPs from the film matrix into the solution. The slower release rate limits the direct contact and antibacterial interaction between CuNPs and bacterial cells in suspension, resulting in lower growth inhibition efficacy [55, 61].

Besides the bond strength, the stability of the antibacterial activity of the metal nanocomposite films is partly influenced by the solubility of the agarose matrix when immersed in aqueous media. Agarose is a highly hydrophilic, water-soluble polymer, suggesting that water infiltration and incubation media can degrade the film structure over time. This effect occurs more rapidly at higher solubility levels, accelerating the dissolution of the matrix and the release of embedded silver and copper ions into the surrounding liquid. While controlled release of antimicrobial ions is desirable, excessively rapid metal ion leakage beyond a critical threshold concentration may conversely reduce long-term antibacterial potency [62].

The antibacterial diffusion tests against *Staphylococcus aureus* showed that Ag-agarose films with 69.34% solubility demonstrated optimal inhibition efficacy at 8 h of incubation. In comparison, Cu-agarose films with slightly lower solubility (59.58%) maintained optimal antibacterial performance for up to 10 h. These observations highlight that solubility and matrix degradation kinetics must be carefully balanced. An ideal solubility profile should facilitate controlled, sustained release of antibacterial ions from nanocomposites over extended periods, ensuring that maximum bactericidal concentrations are reached to preserve efficacy.

4- Conclusion

Using the solution casting method, antibacterial films were successfully prepared using agarose isolated from *Gracilaria sp.* combined with glycerol. The isolated agarose exhibited physicochemical properties similar to those of commercial agarose, with a sulfate content of 0.29%, a melting point of 91°C, a gel-forming temperature of 36.5°C, and an IR spectrum comparable to that of commercial agarose. These findings suggest that this locally sourced agarose could be a viable alternative raw material for various biotechnological and industrial applications.

The incorporation of glycerol and metal nanoparticles enhanced the film formulation. Glycerol, a natural plasticizer, was added to improve flexibility by filling the voids between agarose chains and minimizing irregular aggregation. This resulted in a smoother, more homogeneous film surface with a reduced likelihood of wrinkle formation. Moreover, adding metal nanoparticles further improved the film's mechanical properties by increasing stiffness and tensile strength. According to FESEM and FTIR analyses, AgNPs interact with agarose predominantly through physical bonding, whereas CuNPs engage in coordination bonding with the polymer matrix. These interactions contribute significantly to the overall structural integrity of the films.

Antibacterial assessments demonstrated that the Ag-agarose film effectively inhibited the growth of *Escherichia coli, Salmonella typhimurium, Staphylococcus aureus, Staphylococcus epidermidis,* and *Bacillus subtilis*. In contrast, the Cuagarose film exhibited selective antibacterial activity, specifically inhibiting *Staphylococcus aureus*. These results indicate that agarose-based antibacterial films, primarily developed from locally sourced agarose from Gracilaria sp., hold great promise for food packaging, pharmaceuticals, and other industrial applications. The utilization of indigenous macroalgae provides an economical and sustainable alternative to commercial agarose and enhances the practical use of local marine resources.

5- Declarations

5-1-Author Contributions

Conceptualization, A.K., B.S., R.A.E., R.K., and A.A.; methodology, A.K., B.S., R.A.E., R.K., and A.A.; formal analysis, H.K., H.N., and R.A.; data curation, H.K., H.N., and R.A.; writing—original draft preparation, R.Z., S.H.A., D.Z., and R.A.E.; writing—review and editing, A.K., B.S., R.A.E., R.K., H.K., H.N., D.Z., and A.A.; funding acquisition, B.S. All authors have read and agreed to the published version of the manuscript.

5-2-Data Availability Statement

The findings of this study are supported by data presented in various tables throughout the manuscript. These datasets encompass chemical composition, physical properties, spectral analyses, and antibacterial activity assessments, all of which are essential for developing and characterizing agarose-based nanocomposite films. A summary of the data, along

with its accessibility, is provided in Table S1 for clarity. The datasets and code generated and analyzed during this study have been deposited in Zenodo and are publicly accessible. Table S1 contains details about the datasets, including access links. The datasets and code version used in this study are v1.0, with data accessed on December 28, 2024. Readers can contact the first author at "ahyarahmad@unhas.ac.id" for further information or additional data.

Table S1. Data Access Information for Figures and Tables

Dataset	Repository	DOI/URL	Version	Access Date
Chemical Composition Data	Zenodo	https://doi.org/10.5281/zenodo.14566147	V1.0	December 28, 2024
Physical Properties of Agarose	Zenodo	https://doi.org/10.5281/zenodo.14566164	V1.0	December 28, 2024
FTIR Spectral Data	Zenodo	https://doi.org/10.5281/zenodo.14566174	v1.0	December 28, 2024
Sulfate Content Comparison	Zenodo	https://doi.org/10.5281/zenodo.14566185	v1.0	December 28, 2024
Physical Properties of Nanocomposite Films	Zenodo	https://doi.org/10.5281/zenodo.14566193	v1.0	December 28, 2024
Antibacterial Activity Data	Zenodo	https://doi.org/10.5281/zenodo.14566209	v1.0	December 28, 2024

5-3- Funding and Acknowledgements

The authors sincerely thank the dedicated staff of the Biochemistry Laboratory at Hasanuddin University, Indonesia, for their invaluable support and expertise. We would also like to thank the facilities and scientific and technical support from the Advanced Characterization Laboratory - Integrated Laboratory of Bioproducts, the Research Center for Biomass and Bioproducts, and the National Research and Innovation Agency BRIN. This research was funded by Riset dan Inovasi untuk Indonesia Maju (RIIM) Gelombang 1 Research Program under contract No. B-803/II.7.5/FR/6/2022 and No. B-1373/III.5/PR.03.08/6/2022. It was also partially supported by the Institute for Research and Community Services, Hasanuddin University, through the PFK 2024 fiscal year program under contract No. 00309/UN4.22/PT.01.03/2024.

5-4-Institutional Review Board Statement

Not applicable.

5-5-Informed Consent Statement

Not applicable.

5-6-Conflicts of Interest

The authors declare that there is no conflict of interest regarding the publication of this manuscript. In addition, the ethical issues, including plagiarism, informed consent, misconduct, data fabrication and/or falsification, double publication and/or submission, and redundancies have been completely observed by the authors.

6- References

- [1] Mahmud, N., Islam, J., & Tahergorabi, R. (2021). Marine biopolymers: Applications in food packaging. Processes, 9(12), 1–34. doi:10.3390/pr9122245.
- [2] Krishnan, L., Ravi, N., Kumar Mondal, A., Akter, F., Kumar, M., Ralph, P., & Kuzhiumparambil, U. (2024). Seaweed-based polysaccharides review of extraction, characterization, and bioplastic application. Green Chemistry, 26(10), 5790–5823. doi:10.1039/d3gc04009g.
- [3] Fu, L., Xiao, Q., Ru, Y., Hong, Q., Weng, H., Zhang, Y., Chen, J., & Xiao, A. (2024). Bio-based active packaging: Gallic acid modified agarose coatings in grass carp (Ctenopharyngodon idellus) preservation. International Journal of Biological Macromolecules, 255, 128196. doi:10.1016/j.ijbiomac.2023.128196.
- [4] Zarrintaj, P., Manouchehri, S., Ahmadi, Z., Saeb, M. R., Urbanska, A. M., Kaplan, D. L., & Mozafari, M. (2018). Agarose-based biomaterials for tissue engineering. Carbohydrate Polymers, 187, 66–84. doi:10.1016/j.carbpol.2018.01.060.
- [5] Atef, M., Rezaei, M., & Behrooz, R. (2015). Characterization of physical, mechanical, and antibacterial properties of agar-cellulose bionanocomposite films incorporated with savory essential oil. Food Hydrocolloids, 45, 150–157. doi:10.1016/j.foodhyd.2014.09.037.
- [6] Kajla, P., Chaudhary, V., Dewan, A., Bangar, S. P., Ramniwas, S., Rustagi, S., & Pandiselvam, R. (2024). Seaweed-based biopolymers for food packaging: A sustainable approach for a cleaner tomorrow. International Journal of Biological Macromolecules, 274, 133166. doi:10.1016/j.ijbiomac.2024.133166.

- [7] Khodashenas, B. (2016). The Influential Factors on Antibacterial Behaviour of Copper and Silver Nanoparticles. Indian Chemical Engineer, 58(3), 224–239. doi:10.1080/00194506.2015.1026950.
- [8] Zia, R., Riaz, M., Farooq, N., Qamar, A., & Anjum, S. (2018). Antibacterial activity of Ag and Cu nanoparticles synthesized by chemical reduction method: A comparative analysis. Materials Research Express, 5(7), 1–7. doi:10.1088/2053-1591/aacf70.
- [9] Bruna, T., Maldonado-Bravo, F., Jara, P., & Caro, N. (2021). Silver nanoparticles and their antibacterial applications. International Journal of Molecular Sciences, 22(13), 1–21. doi:10.3390/ijms22137202.
- [10] Onofre-Cordeiro, N. A., Silva, Y. E. O., Solidônio, E. G., de Sena, K. X. F. R., Silva, W. E., Santos, B. S., Aquino, K. A. S., Lima, C. S. A., & Yara, R. (2018). Agarose-silver particles films: Effect of calcium ascorbate in nanoparticles synthesis and film properties. International Journal of Biological Macromolecules, 119, 701–707. doi:10.1016/j.ijbiomac.2018.07.115.
- [11] Gholinejad, M., & Jeddi, N. (2014). Copper nanoparticles supported on agarose as a bioorganic and degradable polymer for multicomponent click synthesis of 1,2,3-triazoles under low copper loading in water. ACS Sustainable Chemistry & Engineering, 2(12), 2658–2665. doi:10.1021/sc500395b.
- [12] Zhang, Y., Fu, X., Duan, D., Xu, J., & Gao, X. (2019). Preparation and characterization of agar, agarose, and agaropectin from the red alga Ahnfeltia plicata. Journal of Oceanology and Limnology, 37(3), 815–824. doi:10.1007/s00343-019-8129-6.
- [13] Pramasari, D. A., Sondari, D., Rachmawati, S. A., Ningrum, R. S., & Sufiandi, S. (2021). The effect of alkaline-autoclaving delignification on chemical component changes of sugarcane trash. IOP Conference Series: Earth and Environmental Science, 759(1), 1–8. doi:10.1088/1755-1315/759/1/012010.
- [14] Zucca, P., Fernandez-Lafuente, R., & Sanjust, E. (2016). Agarose and its derivatives as supports for enzyme immobilization. Molecules, 21(11). doi:10.3390/molecules21111577.
- [15] Aslinda, W., & Ahmad, A. (2016). Isolation and Characterization of Agarose from Red Macroalgae Euchema Cottoni for DNA Fragment Separation. Natural Science: Journal of Science and Technology, 5(3), 307-313. doi:10.22487/25411969.2016.v5.i3.7214.
- [16] Gilcreas, F. W. (1966). Standard methods for the examination of water and waste water. American Journal of Public Health and the Nations Health, 56(3), 387-388.
- [17] Gu, Y., Cheong, K. L., & Du, H. (2017). Modification and comparison of three Gracilaria spp. agarose with methylation for promotion of its gelling properties. Chemistry Central Journal, 11(1), 2–10. doi:10.1186/s13065-017-0334-9.
- [18] Rice, E. W., Baird, R. B., & Eaton, A. D. (2017). Standard Methods for the Examination of Water and Wastewater (23rd Ed.). American Public Health Association (APHA), Washington, United States.
- [19] Njoki, P. N. (2019). Transformation of Silver Nanoparticles in Phosphate Anions: An Experiment for High School Students. Journal of Chemical Education, 96(3), 546–552. doi:10.1021/acs.jchemed.8b00602.
- [20] Iwuji, C., Saha, H., Ghann, W., Dotson, D., Bhuiya, M. A. K., Parvez, M. S., Jahangir, Z. S., Rahman, M. M., Chowdhury, F. I., & Uddin, J. (2024). Synthesis and characterization of silver nanoparticles and their promising antimicrobial effects. Chemical Physics Impact, 9, 100758. doi:10.1016/j.chphi.2024.100758.
- [21] Asmat-Campos, D., Delfin-Narciso, D., Juárez-Cortijo, L., & Nazario-Naveda, R. (2021). Influence of the volume of ascorbic acid in the synthesis of copper nanoparticles mediated by chemical pathway and its stability over time. IOP Conference Series: Earth and Environmental Science, 897(1), 1–8. doi:10.1088/1755-1315/897/1/012010.
- [22] Tantra, R., Schulze, P., & Quincey, P. (2010). Effect of nanoparticle concentration on zeta-potential measurement results and reproducibility. Particuology, 8(3), 279–285. doi:10.1016/j.partic.2010.01.003.
- [23] Ediyilyam, S., George, B., Shankar, S. S., Dennis, T. T., Wacławek, S., Černík, M., & Padil, V. V. T. (2021). Chitosan / Gelatin / Silver Nanoparticles Composites Films for Biodegradable Food Packaging Applications. Polymers, 13(11), 1680. doi:10.3390/polym13111680.
- [24] ASTM E2015-04(2021). (2025). Guide for Preparation of Plastics and Polymeric Specimens for Microstructural Examination. ASTM International, Pennsylvania, United States. doi:10.1520/E2015-04R21.
- [25] ASTM D882-18. (2018). Standard Test Method for Tensile Properties of Thin Plastic Sheeting, ASTM International, Pennsylvania, United States. doi:10.1520/D0882-18.
- [26] Suryanegara, L., Fatriasari, W., Zulfiana, D., Anita, S. H., Masruchin, N., Gutari, S., & Kemala, T. (2021). Novel antimicrobial bioplastic based on PLA-chitosan by addition of TiO₂ and ZnO. Journal of Environmental Health Science and Engineering, 19(1), 415–425. doi:10.1007/s40201-021-00614-z.
- [27] SNI 2690: 2015. (2015). Dried seaweed. Badan Standarisasi Nasional (BSN), Jakarta, Indonesia. (In Indonesian).
- [28] Freile-Pelegrín, Y., & Murano, E. (2005). Agars from three species of Gracilaria (Rhodophyta) from Yucatán Peninsula. Bioresource Technology, 96(3), 295–302. doi:10.1016/j.biortech.2004.04.010.

- [29] Meena, R., Siddhanta, A. K., Prasad, K., Ramavat, B. K., Eswaran, K., Thiruppathi, S., Ganesan, M., Mantri, V. A., & Rao, P. V. S. (2007). Preparation, characterization and benchmarking of agarose from Gracilaria dura of Indian waters. Carbohydrate Polymers, 69(1), 179–188. doi:10.1016/j.carbpol.2006.09.020.
- [30] Lee, W.-K., Lim, Y.-Y., Leow, A. T.-C., Namasivayam, P., Abdullah, J. O., & Ho, C.-L. (2016). Factors affecting yield and gelling properties of agar. Journal of Applied Phycology, 29(3), 1527–1540. doi:10.1007/s10811-016-1009-y.
- [31] Vuai, S. A. H., & Mpatani, F. (2019). Optimization of agar extraction from local seaweed species, Gracilaria salicornia in Tanzania. Phycological Research, 67(4), 261–266. doi:10.1111/pre.12380.
- [32] Ghannadi, A., Shabani, L., & Yegdaneh, A. (2016). Cytotoxic, antioxidant and phytochemical analysis of Gracilaria species from Persian Gulf. Advanced Biomedical Research, 5(1), 1–5. doi:10.4103/2277-9175.187373.
- [33] Mollet, J. C., Rahaoui, A., & Lemoine, Y. (1998). Yield, chemical composition and gel strength of agarocolloids of Gracilaria gracilis, Gracilariopsis longissima and the newly reported Gracilaria cf. vermiculophylla from Roscoff (Brittany, France). Journal of Applied Phycology, 10(1), 59–66. doi:10.1023/A:1008051528443.
- [34] Sharma, M., Prakash Chaudhary, J., Mondal, D., Meena, R., & Prasad, K. (2015). A green and sustainable approach to utilize bio-ionic liquids for the selective precipitation of high purity agarose from an agarophyte extract. Green Chemistry, 17(5), 2867–2873. doi:10.1039/c4gc02498b.
- [35] Jamkhande, P. G., Ghule, N. W., Bamer, A. H., & Kalaskar, M. G. (2019). Metal nanoparticles synthesis: An overview on methods of preparation, advantages and disadvantages, and applications. Journal of Drug Delivery Science and Technology, 53(101174), 1–11. doi:10.1016/j.jddst.2019.101174.
- [36] Ejaz, U., Afzal, M., Mazhar, M., Riaz, M., Ahmed, N., Rizg, W. Y., Alahmadi, A. A., Badr, M. Y., Mushtaq, R. Y., & Yean, C. Y. (2024). Characterization, Synthesis, and Biological Activities of Silver Nanoparticles Produced via Green Synthesis Method Using Thymus Vulgaris Aqueous Extract. International Journal of Nanomedicine, 19, 453–469. doi:10.2147/IJN.S446017.
- [37] Zakir, M., Maming, M., Lembang, M. S., & Lembang, E. Y. (2021). Reduction mechanisms of Ag(I) and Au(III) in the synthesis of silver and gold nanoparticles using leaf extract of Terminalia catappa. Jurnal Natural, 21(2), 89-98. doi:10.24815/jn.v21i2.20677.
- [38] Patil, R. B., & Chougale, A. D. (2021). Analytical methods for the identification and characterization of silver nanoparticles: A brief review. Materials Today: Proceedings, 47, 5520–5532. doi:10.1016/j.matpr.2021.03.384.
- [39] Khatoon, U. T., Nageswara Rao, G. V. S., & Mohan, M. K. (2013). Synthesis and characterization of copper nanoparticles by chemical reduction method. International Conference on Advanced Nanomaterials & Emerging Engineering Technologies, 11–14. doi:10.1109/icanmeet.2013.6609221.
- [40] Tessema, B., Gonfa, G., Hailegiorgis, S. M., Prabhu, S. V., & Manivannan, S. (2023). Synthesis and characterization of silver nanoparticles using reducing agents of bitter leaf (Vernonia amygdalina) extract and tri-sodium citrate. Nano-Structures & Nano-Objects, 35, 100983. doi:10.1016/j.nanoso.2023.100983.
- [41] Sadia, B. O., Cherutoi, J. K., & Achisa, C. M. (2021). Optimization, Characterization, and Antibacterial Activity of Copper Nanoparticles Synthesized Using Senna didymobotrya Root Extract. Journal of Nanotechnology, 2021(1), 5611434. doi:10.1155/2021/5611434.
- [42] Antonio-Pérez, A., Durán-Armenta, L. F., Pérez-Loredo, M. G., & Torres-Huerta, A. L. (2023). Biosynthesis of Copper Nanoparticles with Medicinal Plants Extracts: From Extraction Methods to Applications. Micromachines, 14(10), 1882. doi:10.3390/mi14101882.
- [43] Mohd Amin, A. M., Mohd Sauid, S., Musa, M., & Ku Hamid, K. H. (2017). The Effect of Glycerol Content on Mechanical Properties, Surface Morphology and Water Absorption of Thermoplastic Films From Tacca Leontopetaloides Starch. Jurnal Teknologi, 79(5–3), 11327. doi:10.11113/jt.v79.11327.
- [44] Tarique, J., Sapuan, S. M., & Khalina, A. (2021). Effect of glycerol plasticizer loading on the physical, mechanical, thermal, and barrier properties of arrowroot (Maranta arundinacea) starch biopolymers. Scientific Reports, 11(1), 13900. doi:10.1038/s41598-021-93094-y.
- [45] Medina, I., Scholl, S., & Rädle, M. (2022). Film Thickness and Glycerol Concentration Mapping of Falling Films Based on Fluorescence and Near-Infrared Technique. Micromachines, 13(12), 2184. doi:10.3390/mi13122184.
- [46] JIS Z 1707:2019. (2019). General Rules of Plastic Films for Food Packaging. Japanese Standards Association, Tokyo, Japan.
- [47] ASTM D6988-08. (2013). Standard Guide for Determination of Thickness of Plastic Film Test Specimens. ASTM International, Pennsylvania, United States. doi:10.1520/D6988-08.
- [48] Lian, H., Shi, J., Zhang, X., & Peng, Y. (2020). Effect of the added polysaccharide on the release of thyme essential oil and structure properties of chitosan based film. Food Packaging and Shelf Life, 23, 100467. doi:10.1016/j.fpsl.2020.100467.
- [49] Perdones, Á., Chiralt, A., & Vargas, M. (2016). Properties of film-forming dispersions and films based on chitosan containing basil or thyme essential oil. Food Hydrocolloids, 57, 271–279. doi:10.1016/j.foodhyd.2016.02.006.

- [50] Fadhila G.S, A. A., Darwis, W., Wibowo, R. H., Sipriyadi, S., & Supriati, R. (2021). Antibacterial Activity of the Ethanolic Extract of Sembung Rambat (Mikania micrantha Kunth) Leaves Against Bacillus subtilis. Natural Science: Journal of Science and Technology, 10(1), 6–11. doi:10.22487/25411969.2021.v10.i1.15476.
- [51] Suyatma, N. E., Tighzert, L., Copinet, A., & Coma, V. (2005). Effects of hydrophilic plasticizers on mechanical, thermal, and surface properties of chitosan films. Journal of Agricultural and Food Chemistry, 53(10), 3950–3957. doi:10.1021/jf048790+.
- [52] Ojagh, S. M., Rezaei, M., Razavi, S. H., & Hosseini, S. M. H. (2010). Development and evaluation of a novel biodegradable film made from chitosan and cinnamon essential oil with low affinity toward water. Food Chemistry, 122(1), 161–166. doi:10.1016/j.foodchem.2010.02.033.
- [53] Bang, Y. J., Roy, S., & Rhim, J. W. (2022). A Facile In Situ Synthesis of Resorcinol-Mediated Silver Nanoparticles and the Fabrication of Agar-Based Functional Nanocomposite Films. Journal of Composites Science, 6(5), 1–14. doi:10.3390/jcs6050124.
- [54] Saravanan, B., & Manivannan, V. (2018). Synthesis of copper nanoparticles using trisodium citrate and evaluation of antibacterial activity. Research Journal of Life Sciences, Bioinformatics, Pharmaceutical and Chemical Sciences, 4(5), 841–849. doi:10.26479/2018.0405.60.
- [55] Rhim, J. W., Wang, L. F., & Hong, S. I. (2013). Preparation and characterization of agar/silver nanoparticles composite films with antimicrobial activity. Food Hydrocolloids, 33(2), 327–335. doi:10.1016/j.foodhyd.2013.04.002.
- [56] Elango, M., Deepa, M., Subramanian, R., & Mohamed Musthafa, A. (2018). Synthesis, Characterization, and Antibacterial Activity of Polyindole/Ag-Cuo Nanocomposites by Reflux Condensation Method. Polymer - Plastics Technology and Engineering, 57(14), 1440–1451. doi:10.1080/03602559.2017.1410832.
- [57] Shankar, S., Teng, X., & Rhim, J. W. (2014). Properties and characterization of agar/CuNP bionanocomposite films prepared with different copper salts and reducing agents. Carbohydrate Polymers, 114, 484–492. doi:10.1016/j.carbpol.2014.08.036.
- [58] Girma, A., Alamnie, G., Bekele, T., Mebratie, G., Mekuye, B., Abera, B., Workineh, D., Tabor, A., & Jufar, D. (2024). Greensynthesised silver nanoparticles: antibacterial activity and alternative mechanisms of action to combat multidrug-resistant bacterial pathogens: a systematic literature review. Green Chemistry Letters and Reviews, 17(1), 2412601. doi:10.1080/17518253.2024.2412601.
- [59] Hajipour, M. J., Fromm, K. M., Akbar Ashkarran, A., Jimenez de Aberasturi, D., Larramendi, I. R. de, Rojo, T., Serpooshan, V., Parak, W. J., & Mahmoudi, M. (2012). Antibacterial properties of nanoparticles. Trends in Biotechnology, 30(10), 499–511. doi:10.1016/j.tibtech.2012.06.004.
- [60] Soldatović, T. (2021). Correlation between HSAB Principle and Substitution Reactions in Bioinorganic Reactions. Photophysics, Photochemical and Substitution Reactions - Recent Advances. IntechOpen Limited, London, United Kingdom. doi:10.5772/intechopen.91682.
- [61] Rhim, J. W., Gennadios, A., Handa, A., Weller, C. L., & Hanna, M. A. (2000). Solubility, tensile, and color properties of modified soy protein isolate films. Journal of Agricultural and Food Chemistry, 48(10), 4937–4941. doi:10.1021/jf0005418.
- [62] Kanmani, P., & Rhim, J. W. (2014). Antimicrobial and physical-mechanical properties of agar-based films incorporated with grapefruit seed extract. Carbohydrate Polymers, 102(1), 708–716. doi:10.1016/j.carbpol.2013.10.099.